Available online at www.sciencedirect.com
SCIENCE DIRECT
Journal of Catalysis 227 (2004) 304–312
JOURNAL OF CATALYSIS
www.elsevier.com/locate/jcat

Catalytic oxidation of benzene with ozone over alumina-supported manganese oxides

Hisahiro Einaga *, Shigeru Futamura

National Institute of Advanced Industrial Science and Technology, AIST Tsukuba West, 16-1, Onogawa, Tsukuba, Ibaraki 305-8569, Japan

Received 21 May 2004; revised 25 July 2004; accepted 28 July 2004

Available online 26 August 2004

Abstract

Catalytic oxidation of benzene with ozone over alumina-supported manganese oxides was carried out at room temperature (295 K) to investigate the behavior of benzene oxidation and CO_x formation. The ratio of the decomposition rate for ozone to that for benzene was found to be 6, independent of ozone concentration, reaction times, and the amount of Mn loading. A linear correlation was observed for the amount of ozone decomposed and that of CO_x formed, whereas deviation from linearity was observed between the amount of ozone decomposed and that of benzene reacted. Carbon balance was in the range of 26–37% due to the formation of two types of intermediates, weakly bound compounds including formic acid and strongly bound surface formate and carboxylates. Catalyst was significantly deactivated due to the buildup of the intermediates on the catalyst surface during the course of benzene oxidation. The weakly bound compounds were removed by heat treatment at 573 K in the O_2 flow. The strongly bound surface formate and carboxylates were oxidized to CO_x by further heating up to 723 K. The deactivated catalyst was regenerated by the heat treatment.

Keywords: Benzene oxidation; Catalytic ozonation; Manganese oxide; Catalyst deactivation; Catalyst regeneration

1. Introduction

Ozone is widely used for various industrial and environmental processes, and its reactivity toward organic compounds has been extensively studied both in the liquid phase [1,2] and in the gaseous phase [3]. Catalytic oxidation reactions using ozone are promising technologies for the treatment of air polluted with hazardous compounds [4–6]. Hitherto, the reactions have been reported for the oxidation of CO [7,8], methane [9], alkanes [10], aromatic compounds [11–15], acrylonitrile [15], alcohols [15–17], and chlorohydrocarbons [15,18].

Benzene is one of the hazardous compounds removed from flue gases due to its carcinogenicity. Generally, the elements of the first transition series have been used for the catalytic oxidation of benzene with ozone. Naydenov and Mehandjiev have used unsupported manganese oxides as the catalysts to investigate the effect of the reaction temperature on the rate of benzene oxidation [12]. The use of ozone can lower the reaction temperature for benzene oxidation over manganese oxides. They have also reported that apparent activation energy estimated in the presence of ozone is three times lower than that in the absence of ozone. The mixed oxide catalysts, such as alumina-supported Cu–Cr and Co–Cr [13], $NiMnO_3$-ilmenite, and $NiMn_2O_4$-spinel [14] have also been reported to be effective for benzene oxidation with ozone.

Oyama and his co-workers have mainly studied the ozone decomposition on supported-manganese oxides in the absence of organic substrates [4–6,19–24]. The reaction mechanism was clarified by in situ Raman spectroscopy, ab initio molecular orbital calculations, and kinetic studies [19,20]. They have also used temperature-programmed oxygen desorption techniques and EXAFS studies to determine the structure of the manganese active centers on the supports [21,22]. On the other hand, we have investigated the oxida-

* Corresponding author.
E-mail address: h-einaga@aist.go.jp (H. Einaga).

0021-9517/$ – see front matter
doi:10.1016/j.jcat.2004.07.029

tion of benzene and cyclohexane with ozone over alumina-supported metal oxides, and have reported that manganese oxide showed higher activity than the oxides of Fe, Co, Ni, Cu, and Ag [25].

We herein report the catalytic oxidation of benzene with ozone over supported manganese oxide catalysts at room temperature. Our attention is concentrated on the behavior of benzene oxidation, ozone decomposition, and product formation on the manganese oxide catalysts. Alumina is used as a catalyst support based on the high reactivity of manganese oxides on the support for ozone decomposition [21]. In addition, manganese oxide can be highly dispersed on γ-alumina at low loading levels [26–29].

2. Experimental

2.1. Catalyst materials

Alumina-supported manganese oxides were prepared by the impregnation of γ-Al_2O_3 (Catalysis Society of Japan, JRC ALO-4, S_{BET} 170 $m^2\,g^{-1}$) with the aqueous solution containing an appropriate amount of $Mn(CH_3COO)_2 \cdot 4H_2O$ (Wako Pure Chemical, $>99.9\%$). Catalyst samples were dried at 383 K and then calcined at 773 K for 3 h in air. For simplicity, alumina-supported manganese oxide is denoted by MnO_2/Al_2O_3, although the oxidation states of Mn on alumina supports are mixtures of II–IV [26]. For the preparation of MnO_2/SiO_2 and MnO_2/TiO_2, SiO_2 (JRC SiO-1, $S_{BET} = 110\,m^2\,g^{-1}$) and TiO_2 (P25, $S_{BET} = 43\,m^2\,g^{-1}$) were used as the catalyst supports. MnO_2/ZrO_2 was prepared from ZrO_2 ($S_{BET} = 58\,m^2\,g^{-1}$), which had been obtained by the calcination of $Zr(OH)_4$ at 823 K for 3 h in air.

2.2. Catalytic reactions

Catalytic reactions were carried out with a fixed-bed flow reactor. Fig. 1 shows the schematic of the reaction system used in this study. Reaction gases were prepared by benzene in N_2, N_2 ($>99.9995\%$, total hydrocarbon <1 ppm), and O_2 ($>99.9995\%$, total hydrocarbon <1 ppm) in cylinders by using the sets of thermal mass-flow controllers. Ozone was synthesized from O_2 by a silent discharge ozone generator. Prior to the catalytic reaction, the sample in a Pyrex glass reactor was heated at 723 K in O_2 flow. Then, the catalyst was cooled and thermostated at 295 K with a water bath. After the adsorption–desorption equilibrium was achieved for benzene between the catalyst surface and the gas phase, ozone was continuously fed into the reactor. Unless otherwise stated, ozone concentration was 1000 ± 30 ppm. Catalyst weight was generally 20–75 mg and flow rate was 250–1000 ml min^{-1}. Here, weight hourly specific velocity (WHSV) was 200–3000 L $h^{-1}\,g^{-1}$. Analysis of the gas sample was performed with a Fourier-transform infrared spectrophotometer (Perkin-Elmer Spectrum One) equipped with a 2.4 m optical length gas cell (volume 100 ml). The dead volume, namely, the volume of the reactor and apparatus in the reaction system, was smaller than 20 ml and the residence time under the reaction condition was 1.2–5 s. Both benzene oxidation and ozone decomposition did not proceed in the gas phase with an empty reactor. Thus, homogeneous gaseous reaction of benzene with ozone can be neglected. Reaction rates were evaluated under the conditions where the conversions were linear to W/F.

2.3. Other measurements

FTIR spectra were recorded with a Jasco FT-IR480 Plus spectrometer equipped with a TGS detector. Catalyst samples were pressed into thin self-supporting wafers of 10 mm in diameter (ca. 7 mg) and set in an IR cell with KBr windows, which was connected to the flow-type reaction system described above. Prior to the measurements, the sample was preheated at 723 K in O_2 and then cooled to room temperature. The reaction gas containing 100 ppm benzene was fed to the IR cell. After the adsorption–desorption equilibrium was achieved for benzene between the catalyst surface and gas phase, the feed of 1000 ppm ozone was started. The

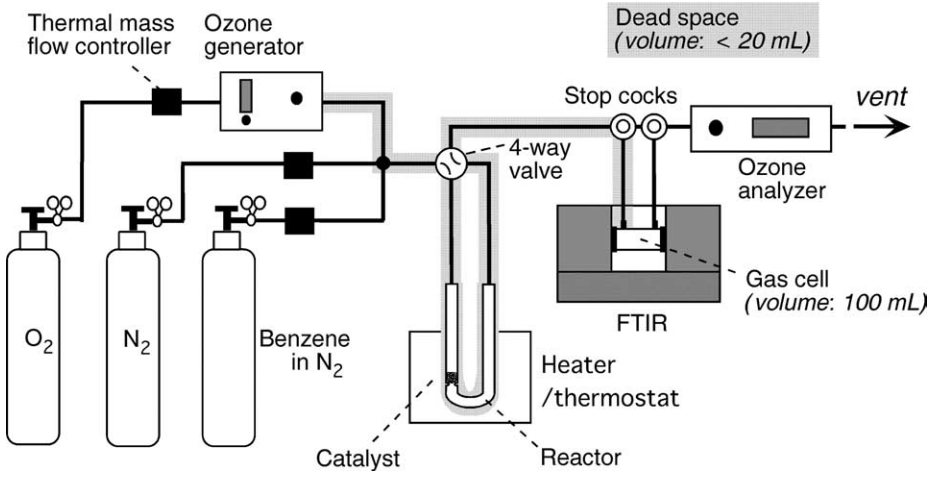

Fig. 1. Schematic of the reaction system for catalytic oxidation by using ozone.

spectra were collected with the resolution of 4 cm^{-1} at room temperature.

Temperature-programmed oxidation was conducted with the flow reactor described above. After the benzene oxidation with ozone was carried out, the reaction gas was switched to N_2–O_2 (9-to-1 in volume) with the flow rate of 500 ml min^{-1}. Then, the used catalyst was heated at a rate of 10 K min^{-1} to 773 K. The effluent gas from the reactor was analyzed by the FTIR spectrometer (Perkin-Elmer Spectrum One) with the 2.4 m optical length gas cell. Product compounds on catalyst surface were determined by a gas chromatograph (Hewlett-Packard 6890) equipped with a mass selective detector (Hewlett-Packard 5973).

3. Results

3.1. Decomposition behavior of benzene on MnO_2/Al_2O_3

Fig. 2 shows the time courses for benzene oxidation and products formation by using ozone with 5 wt% MnO_2/Al_2O_3 catalyst. The conversions of benzene and ozone gradually decreased with time on stream (Stage I in Fig. 2a). CO_2 and CO were observed as the products, and their concentrations also decreased with time. No other products were detected in the gas phase. The mole fraction of CO_2 $[= CO_2/(CO_2 + CO)]$ and the carbon balance were 80 and 30%, respectively, which were almost unchanged during the reaction. After 120 min, the feed of ozone and benzene was stopped, and the reactor was purged out until benzene and CO_x were not observed. When ozone was continuously fed to the reactor without benzene feed (Stage II in Fig. 2a), CO_2 and CO were evolved from the catalyst surface. Their evolution shows that intermediates were deposited on the catalyst surface in the benzene oxidation. The formation rate of CO_2 for the first 10 min in Stage II was higher than that after 120 min in Stage I, indicating that the presence of benzene inhibits the oxidation of the intermediates to CO_2 formation. The mole fraction of CO_2 in this period was higher than that in Stage I. Thus, the fraction in the oxidation of the intermediates is higher than that in benzene oxidation. Carbon balance based on the total amount of CO_x formed and benzene reacted through Stages I and II was 50%. Fig. 2b shows the time course for ozone decomposition in these two stages. The conversion decreased with time on stream in the presence of benzene (Stage I in Fig. 2b). However, no such decrease was observed for ozone conversion after the benzene feed was stopped (Stage II in Fig. 2b).

Table 1 summarizes the results for benzene oxidation with ozone over supported-manganese oxides. Here, the reaction rates were measured 2 h after the reactions were started. When γ-Al_2O_3 without Mn was used for the reaction, the rates for benzene oxidation and ozone decomposition were lower than the limit of experimental error, although the catalyst was slightly browned. No significant difference was observed for the rates by changing the Mn loading of

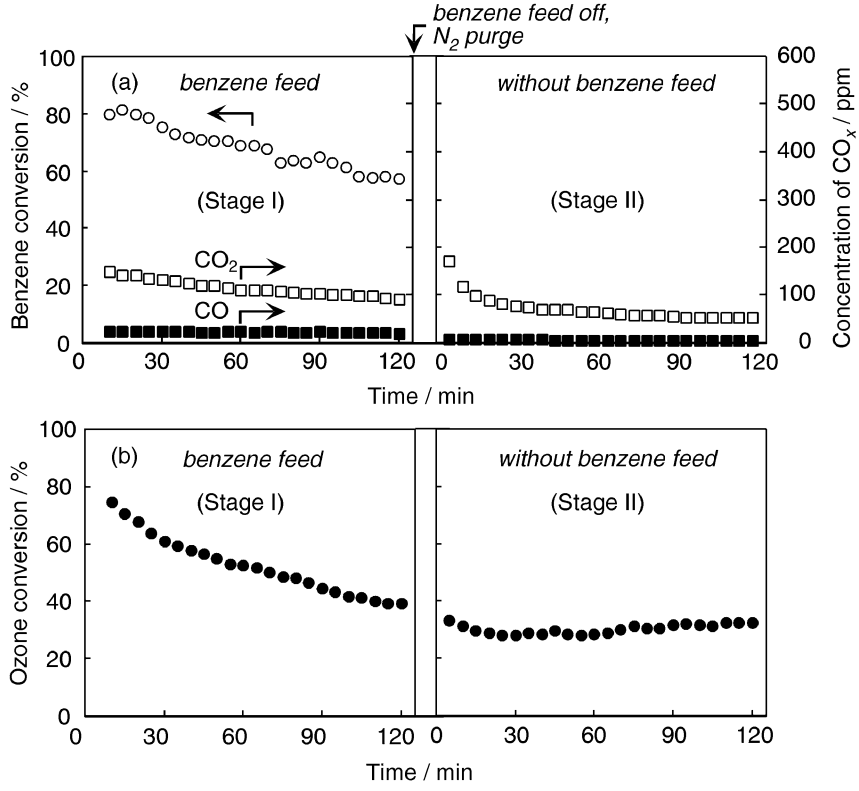

Fig. 2. Time profiles for benzene oxidation, ozone decomposition, and products formation with 5 wt% MnO_2/Al_2O_3. Catalyst 0.05 g, ozone 1000 ppm, oxygen 10%, flow rate 250 ml/min (WHSV 300 L h^{-1} g^{-1}). Benzene: 100 ppm (Stage I); 0 ppm (Stage II).

Table 1
Catalytic activities of supported manganese oxides for benzene oxidation with ozone[a]

Catalyst	Mn loading (%)	Rate[b] (mol min^{-1} g^{-1})		Normalized rate[c] (mol min^{-1} m^{-2})		Surface area[d] (m^2 g^{-1})	Ratio[e]
		Benzene	Ozone	Benzene	Ozone		
γ-Al_2O_3	–	–	–	–	–	170	–
MnO_2/γ-Al_2O_3	5	1.38×10^{-5}	8.29×10^{-5}	8.55×10^{-8}	5.14×10^{-7}	161	6.0
MnO_2/γ-Al_2O_3	10	1.40×10^{-5}	8.46×10^{-5}	9.29×10^{-8}	5.62×10^{-7}	151	6.0
MnO_2/γ-Al_2O_3	20	1.13×10^{-5}	6.50×10^{-5}	7.73×10^{-8}	4.45×10^{-7}	146	5.8
MnO_2/SiO_2	5	1.02×10^{-5}	4.59×10^{-5}	9.66×10^{-8}	4.33×10^{-7}	106	4.5
MnO_2/TiO_2	5	3.09×10^{-6}	2.07×10^{-5}	7.18×10^{-8}	4.82×10^{-7}	43	6.7
MnO_2/ZrO_2	5	3.10×10^{-6}	2.34×10^{-5}	5.41×10^{-8}	4.07×10^{-7}	57	7.5

[a] Conditions: benzene 100 ppm, ozone 1000 ppm, oxygen 10%.
[b] Rate $= C_0 X (W/F)^{-1}$; C_0, initial concentration of benzene or ozone; X, conversion.
[c] Reaction rate normalized by surface area.
[d] Surface area was determined from BET plots. The samples were evacuated ($< 2 \times 10^{-6}$ Torr) at 573 K for 3 h prior to N_2 adsorption measurements.
[e] Ratio of rate for ozone decomposition to that for benzene oxidation. The values were obtained from the slope of the plots between the rates for ozone decomposition and those for benzene oxidation under the conditions where the conversions were linear to W/F.

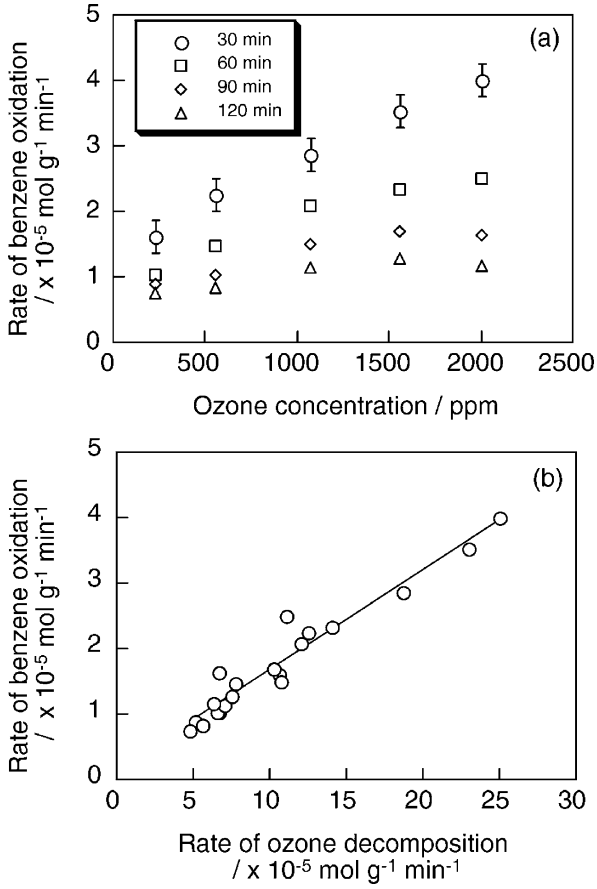

Fig. 3. (a) Effect of ozone concentration of the rate of benzene oxidation at various reaction times. (b) Relationship between the rate of benzene oxidation and that of ozone decomposition. Benzene 100 ppm, ozone 1000 ppm, oxygen 10%. Experimental error: benzene $\pm 0.3 \times 10^{-6}$ mol g^{-1} min^{-1}, ozone $\pm 0.3 \times 10^{-5}$ mol g^{-1} min^{-1}.

MnO_2/Al_2O_3 catalysts from 5 to 20 wt%. In this study, hereafter, the catalyst with 5 wt% was used for the catalytic tests and spectroscopic studies. The ratio of the rate for ozone decomposition to that for benzene oxidation was about 6 for the Al_2O_3-supported catalysts. For comparison, the activities of SiO_2-, TiO_2-, and ZrO_2-supported catalysts are also listed in Table 1. The catalyst supports without manganese oxides were also inactive for the reaction. The rates for benzene oxidation normalized by surface area with SiO_2-, TiO_2-, and ZrO_2-supported catalysts were comparable or slightly lower than those with the Al_2O_3-supported catalysts. The ratio of the rate for ozone decomposition to that for benzene oxidation slightly depended on the support.

Fig. 3a shows the effect of ozone concentration on the rate of benzene oxidation at various reaction times. The oxidation rate at 30 min monotonically increased with the ozone concentration. As the reaction proceeded, the increment of the rate became smaller. At 120 min, the rate was almost saturated at higher concentration levels than 1000 ppm. Fig. 3b shows the relationship between the decomposition rates of benzene and ozone through the reactions at various reaction times. The rate for benzene oxidation increased linearly with that for ozone decomposition. The ratio of the rate for ozone decomposition to that for benzene oxidation was estimated to be 6.1 from the slope, independent of the ozone concentration and the reaction times.

3.2. Formation behavior of CO_x

Fig. 4 shows the dependence of the mole fractions of CO_2 and CO on the benzene conversion. Here, the conversion was varied by changing the WHSV from 200 to 1500 L h^{-1} g^{-1}. The values at 1 and 2 h are plotted in this figure. Both the factions of CO_2 and CO were unchanged in the low conversion region ($< 50\%$). In the higher conversion region, however, the mole fraction of CO_2 increased and that of CO decreased with increasing the conversion. The carbon balance was 26% in the low conversion region and increased slightly in the high conversion region. Fig. 5 shows the relationship between the amount of benzene oxidized and that of CO_x formed and that of ozone reacted. The values at 1 and 2 h are also plotted in this figure. A good linear correlation was observed between the amount of CO_x formed and that of ozone decomposed. According to the slope, the ratio

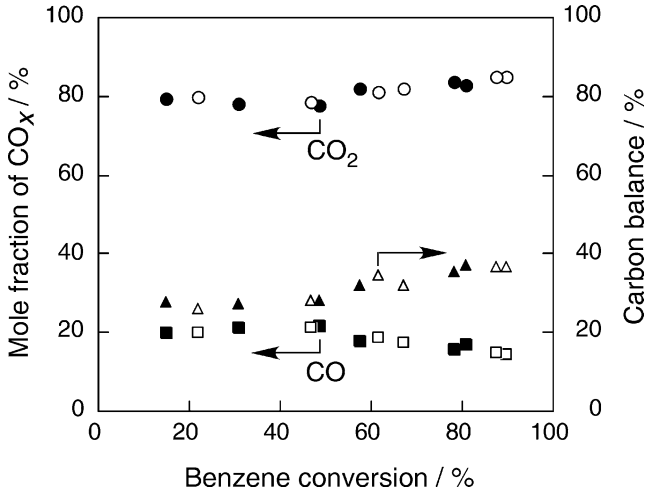

Fig. 4. Dependence of the formation of CO_x and carbon balance on benzene conversion at various WHSV. The values were evaluated at 1 h (○) and 2 h (●). Benzene 100 ppm, ozone 1000 ppm, oxygen 10%.

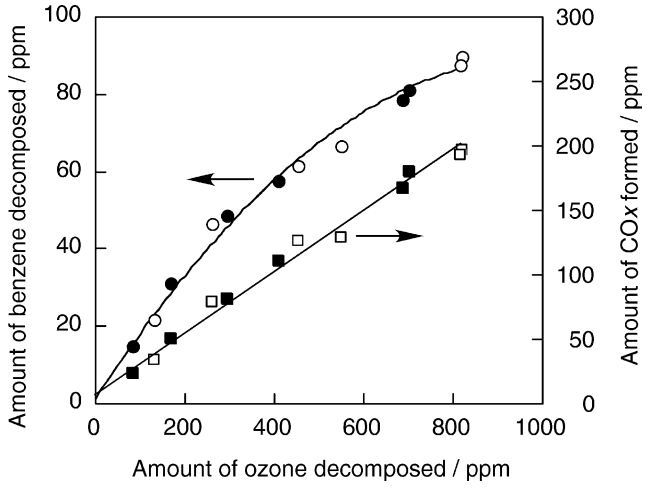

Fig. 5. Relationship between the benzene consumption and CO_x formation with change of ozone consumption. The values were evaluated at 1 h (○) and 2 h (●). Benzene 100 ppm, ozone 1000 ppm, oxygen 10%.

of the amount of ozone decomposed to that of CO_x formed was estimated to be 4.2. On the other hand, deviation from the linearity was observed between the amounts of benzene reacted and that of ozone decomposed in the higher conversion region. The ratio of the amount of benzene oxidized to that of ozone decomposed was estimated to be 6 in the low conversion region and increased to 9 in the high conversion region.

3.3. FTIR spectroscopic studies

Catalytic oxidation reactions were carried out in an FTIR cell at room temperature. Fig. 6a shows the spectra of the catalyst during the benzene oxidation with ozone. The spectra were collected without ozone at first, and then at the intervals of 2–10 min from the start of ozone feed. The spectrum of the catalyst before the reaction exhibited only the

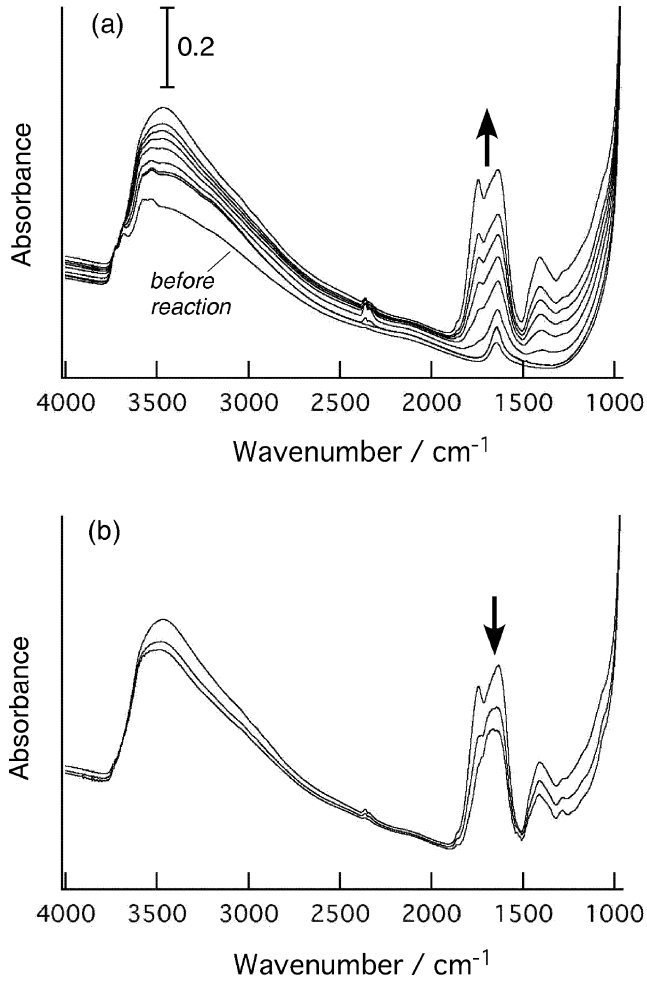

Fig. 6. FTIR spectra of MnO_2/Al_2O_3 catalyst. (a) During the course of benzene oxidation with ozone: benzene 100 ppm, ozone 1000 ppm, oxygen 10%. Spectra were taken after 0, 2, 4, 8, 12, 16, 20, and 30 min. (b) During the ozone feed without benzene: ozone 1000 ppm, oxygen 10%. Spectra were taken after 0, 30, and 120 min.

bands of adsorbed water and hydroxyl groups on the catalyst surface (1620 and 2500–3700 cm^{-1}), even after the catalyst was equilibrated with dilute benzene (100 ppm). No bands assigned to benzene were observed probably due to its low concentration and low absorption coefficiency. When the ozone feed was started, new bands appeared in the range of 1000–1800 cm^{-1} with the maximum intensities at 1412, 1636, and 1754 cm^{-1}. Their intensities monotonically increased with time on stream, indicating that organic by-products were accumulated on the catalyst surface. The band at 1754 cm^{-1} is assigned to the C=O stretching vibration of formic acid on the catalyst surface (see below). The broader band at around 1636 cm^{-1} and the bands at around 1412 cm^{-1} may be the overlapping of several bands including OH bending of adsorbed water and the OH stretching of alcohols and carboxylic acids. The intensity of a broad band in the range of 2500–3700 cm^{-1} assignable to OH stretching of water and/or organic intermediates also increased during the reaction. These bands were not observed in the spectrum

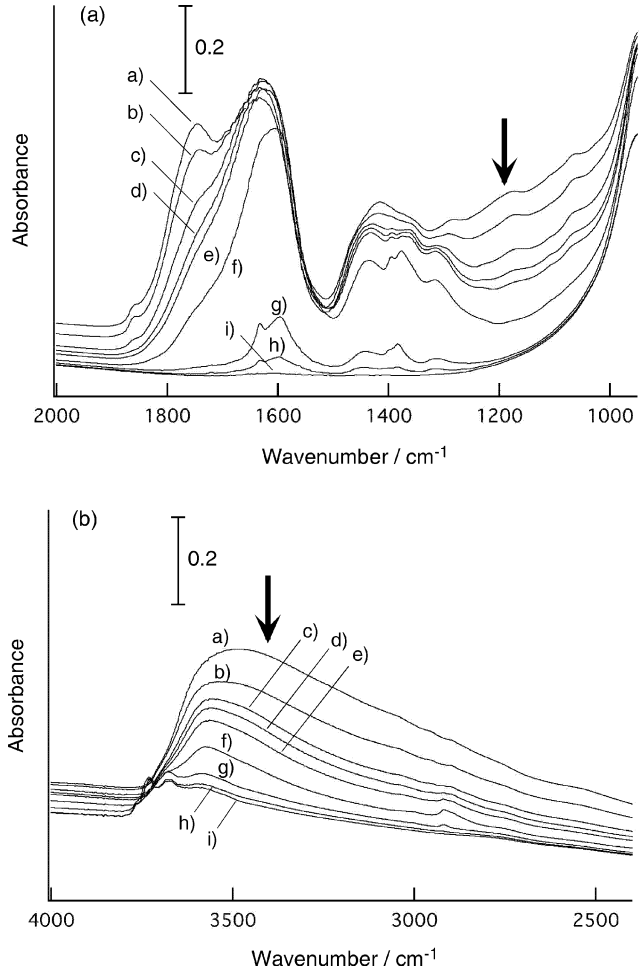

Fig. 7. FTIR spectral changes in MnO_2/Al_2O_3 surface by heating the catalyst in O_2 flow at room temperature (a), 373 K (b), 423 K (c), 473 K (d), 523 K (e), 573 K (f), 623 K (g), 673 K (h), and 723 K (i).

when ozone was contacted with the MnO_2/Al_2O_3 catalyst without benzene, although the data are not shown.

After the benzene oxidation with ozone was conducted, gaseous benzene was purged out and ozone was continuously introduced into the reactor again without benzene feed. As shown in Fig. 6b, the intensity of the newly observed bands gradually decreased with time on stream in the presence of ozone. Especially, the band at 1754 cm^{-1} was greatly diminished after 120 min, while the bands at 1636 and 1412 cm^{-1} and the broad band in the range of 2500–3700 cm^{-1} remained.

Fig. 7 shows the FTIR spectra obtained after the heating of the catalyst in the flow of O_2, which had been used for the benzene oxidation with ozone for 120 min. The catalyst sample was heated for a few minutes at the desired temperature. Spectra were taken after the sample was cooled to room temperature. When the sample was heated to 473 K, the band at 1750 cm^{-1} and that in the range of 1050–1300 cm^{-1} disappeared, while the band at around 1630 cm^{-1} and that at around 1400 cm^{-1} were almost unchanged. The heating up to 573 K decreased the intensity of the band especially in the region of 1620–1780 cm^{-1} and that in the range of 1000–1500 cm^{-1}. Instead, the bands at 1320, 1380, 1400, 1440, and 1610 cm^{-1} appeared. These new bands are assigned to the antisymmetric and symmetric COO– stretching with the CH deformation of the surface formate and carboxylate species [30–32]. Further heating up to 623 K greatly reduced the intensities of the bands of the residual species. On the other hand, the band in the region of 2500–3700 cm^{-1} monotonically decreased in its intensity by increasing the heating temperature. The residual species on the catalyst surface were almost completely removed after the catalyst was heated up to 723 K.

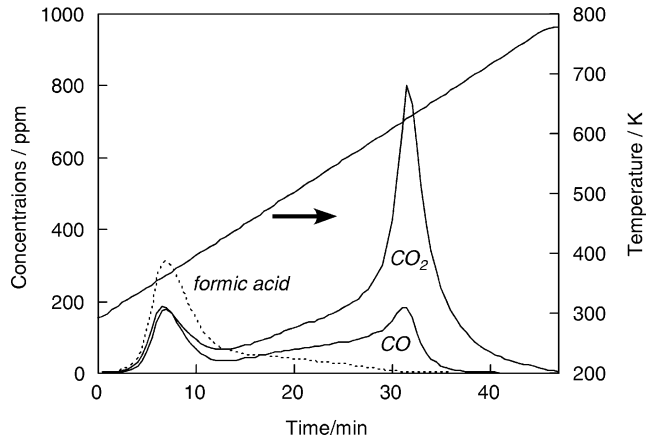

Fig. 8. TPO profiles of the used MnO_2/Al_2O_3 catalyst. Temperature ramp: 10 K min^{-1}.

When the intermediate compounds on the used catalyst were extracted with methanol and analyzed on GC-MS, formic acid was detected as a major by-product. As the minor by-products, 2,5-furandione, phenol, acetic acid, and oxalic acid were also detected. However, these compounds were not detected after the used catalyst was heated at 573 K in the O_2 flow. Thus, the intermediate compounds such as carboxylic acids and phenols on the catalyst were all decomposed by the heating up to 573 K, and the residual formate and carboxylates could not be extracted with the organic solvents.

3.4. Temperature-programmed oxidation

Fig. 8 shows the TPO profiles obtained when the used catalyst was heated from room temperature to 773 K. The catalyst had been used for the benzene oxidation with ozone for 4 h (benzene, 100 ppm; ozone, 1000 ppm; O_2, 10%; WHSV, 1200 L h^{-1} g^{-1}). Formic acid was mainly observed at the temperature region of 300–500 K and was not observed at temperatures higher than 623 K. On the other hand, two peaks were observed for CO_2 at 360 and 620 K. Especially, larger amounts of CO_2 were observed at the temperature range of 573–673 K. The amount of CO was comparable with that of CO_2 in the lower temperature region. However, its amount was much smaller than that of CO_2 in the higher temperature region. According to the TPO pro-

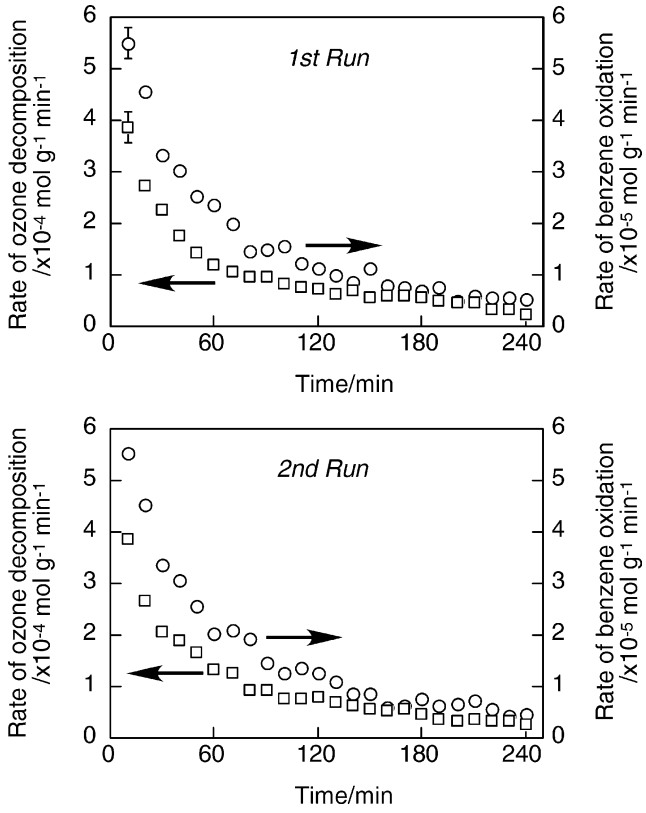

Fig. 9. Time courses for benzene oxidation with ozone over MnO_2/Al_2O_3 catalyst. Benzene 100 ppm, ozone 1000 ppm, oxygen 10%. Experimental error: benzene $\pm 0.3 \times 10^{-6}$ mol g^{-1} min^{-1}, ozone $\pm 0.3 \times 10^{-5}$ mol g^{-1} min^{-1}.

files, the amounts of CO_2, CO, and formic acid were 0.1462, 0.0548, and 0.0465 mmol-C (g-catalyst)$^{-1}$, respectively.

3.5. *Effect of heat treatment on the time course for benzene decomposition with ozone*

Fig. 9 shows the time courses for benzene oxidation with ozone when the catalyst was repeatedly used for the reaction. Both the rates of benzene oxidation and ozone decomposition decreased with time on stream (first run). Steady-state activity was not obtained. After the benzene oxidation was carried out for 4 h, the catalyst was heated in O_2 flow up to 723 K for 1 h. Then, the benzene decomposition was carried out again under the same conditions as those of first run. Almost the same time course plots were obtained for these two reaction profiles. After the 4-h reaction, the total amount of benzene reacted was estimated to be 3.8 ± 0.7 mmol per 1 g of catalyst. By using this value, the turnover number per a Mn site was estimated to be 4.3 ± 0.8, indicating that the reaction catalytically proceeded.

Fig. 10 shows the ozone decomposition with the MnO_2/Al_2O_3 catalyst without benzene feed. No deactivation was observed until 80 min, after which the rate of ozone decomposition slightly decreased with time on stream (Stage I). The decomposition rate at 240 min was 6.3×10^{-4} mol min^{-1} g^{-1}, which corresponded to 0.9 times the rate of

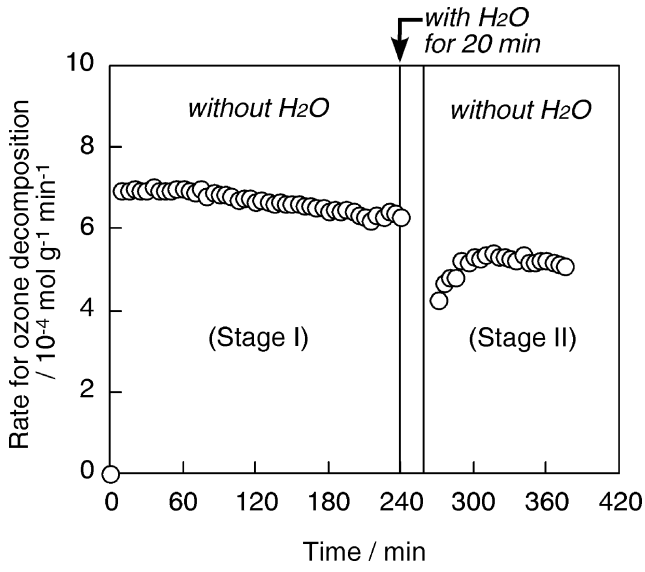

Fig. 10. Effect of water vapor contact on the reaction rate of ozone decomposition with MnO_2/Al_2O_3 catalyst. Benzene 100 ppm, ozone 1000 ppm, oxygen 10% (WHSV 2000 L h^{-1} g^{-1}).

the first 10 min. After the gas saturated with water vapor was fed to the reactor for 20 min, the ozone decomposition was carried out again (Stage II). By this treatment, totally 6.9×10^{-4} mol of water vapor was contacted with the catalyst. The ozone conversion was dropped to the rate of 4.3×10^{-4} mol min^{-1} g^{-1}. However, it increased to 5.1×10^{-4} mol min^{-1} g^{-1} after 300 min, which corresponded to 0.73 times the rate for the first 10 min in Stage I.

4. Discussion

In the present study, we demonstrate that benzene oxidation catalytically proceeds with MnO_2/Al_2O_3 to give CO_2 and CO with the mole fractions of around 80 and 20%, respectively, which slightly depend on reaction conditions. The low carbon balance (26–37%) is ascribed to the formation of intermediates on the catalyst surface in the benzene oxidation. Although Mn is crucial for obtaining catalytic activity, the rate of benzene oxidation is not so much sensitive to the amount of Mn loaded. Our investigation on the effect of the supports reveals that Al_2O_3 is an effective support for manganese oxides in the benzene oxidation with ozone. However, the reaction rate normalized by surface area for SiO_2-supported catalysts is comparable to that for Al_2O_3. In addition, the rates with TiO_2- and ZrO_2-supported catalyst are 20 and 40% lower than those with Al_2O_3-supported catalysts, respectively. Therefore, the surface area of the support is one of the important factors for catalytic activities.

Oyama and his co-workers have investigated the mechanism for O_3 decomposition on manganese oxide supported on Al_2O_3 without organic substrates, and have reported that the reaction proceeds through two irreversible steps, the ad-

sorption of ozone on the catalyst surface and the desorption of molecular oxygen,

$$O_3 + {}^* \rightarrow O_2 + O^*, \quad (1)$$

$$O^* + O_3 \rightarrow O_2 + O_2{}^*, \quad (2)$$

$$O_2{}^* \rightarrow O_2 + {}^*, \quad (3)$$

where * denotes the surface site on the catalyst [19,20]. As the intermediate species, atomic oxygen and peroxides have been observed [19]. Imamura et al. [7] and Naydenov et al. [8] have suggested on the basis of ESR studies that the oxygen anions O^- are formed on Ag_2O and CeO_2 in the presence of ozone and these species oxidize CO and benzene. Such active oxygen species are responsible for benzene oxidation on manganese oxide catalysts.

The ratio of decomposition rate of ozone to benzene is estimated to be 6, and the value does not depend on the ozone concentration, reaction times, or the amount of Mn loading. The value is almost the same as that obtained in the benzene oxidation over other types of metal oxides (Fe, Co, Ni, Cu, and Ag) supported on Al_2O_3 [25]. Thus, the activities for benzene oxidation with ozone strongly depend on those for ozone decomposition. This finding is consistent with the consideration that the active oxygen species formed in ozone decomposition are responsible for benzene oxidation. Based on these findings, the reaction stoichiometry is estimated. If only one atom of O_3 was reacted to oxidize benzene, the reaction equation can be written as

$$C_6H_6 + 15O_3 = 6CO_2 + 3H_2O + 15O_2 \quad (4)$$

according to the reaction mechanism shown in Eqs. (1)–(3). The value of 6 for the ratio of the decomposition rates is lower than that estimated from the above equation ($O_3/C_6H_6 = 15$). This indicates that not only ozone but also molecular oxygen participates as an important role in the benzene decomposition: O_2 may be involved in the autoxidation processes, in which the radical intermediates formed in benzene oxidation are oxidized by O_2

$$R\cdot + O_2 \rightarrow RO_2\cdot \rightarrow CO_2, CO. \quad (5)$$

A linear relationship between the amount of CO_x formed and that of ozone decomposed (Fig. 5) implies that the formation behavior of CO_x is dominated by the decomposition behavior of ozone. On the other hand, deviation from linear plots between the amount of benzene oxidized and that of ozone decomposed can be explained in terms of the following mechanism: ozone is mainly consumed in the benzene oxidation at low conversion levels, while ozone is much more consumed in the oxidation of the intermediates at high conversion levels, which leads to the increase in carbon balance and the mole fraction of CO_2 (Fig. 4). This consideration is supported by the findings that the presence of benzene inhibits the oxidation of intermediates to CO_x, and that the mole fraction of CO_2 in the oxidation of the intermediates is higher than that in benzene oxidation (Fig. 2).

MnO_2/Al_2O_3 catalyst is gradually deactivated during the benzene oxidation due to the buildup of the intermediates on the catalyst surface. Although the rate for ozone decomposition significantly decreased in the benzene oxidation, no such deactivation was observed without benzene feed (Figs. 2 and 10). The accumulation of the organic intermediates is also evidenced by the FTIR spectra, which shows the appearance of new bands in the wavenumber range of 1000–800 and 2500–3700 cm^{-1}. The detection of carboxylic acids, 2,5-furandione and phenol, urged us to assign these bands to the overlapping of the stretching and the bending of oxygen-containing groups, –C=O, –OH, and –C–O–. The bands at 1754 and 1100 cm^{-1} are assigned to formic acid on the catalyst surface [32]. The disappearance of these bands during the ozone feed without benzene is also consistent with the finding that the organic intermediates are decomposed in the reaction with ozone.

According to the stoichiometry described in Eq. (4), three molecules of water are formed when one molecules of benzene is completely oxidized. Our results show that the adsorbed water on the catalyst surface also inhibits the benzene oxidation on active sites. After 6.9×10^{-4} mol of water vapor (corresponding to 53 times the amount of Mn sites on the catalyst surface) was contacted with catalyst surface, the rate of ozone decomposition decreased to around 0.5 times the initial reaction rate (Fig. 10). However, the rate of ozone decomposition was recovered to some extent after the feed of water vapor was stopped, very probably due to the desorption of adsorbed water. Thus, adsorbed water is not the dominant factor for the severe deactivation of MnO_2/Al_2O_3 catalyst in the benzene oxidation.

FTIR studies combined with TPO measurements provide further information on the intermediates on the MnO_2/Al_2O_3 catalyst. By heating the catalyst up to 423 K, formic acid on the catalyst surface was desorbed from the catalyst surface and the band at 1754 cm^{-1} and around 1100 cm^{-1} disappeared, which confirms the assignment of these two bands to formic acid. The weakly bound intermediates including formic acid, carboxylic acids, 2,5-furanedione, and phenol were completely decomposed by the subsequent heating up to 573 K. The new bands due to strongly bound surface formate and carboxylates remained on the catalyst surface, which give the bands of 1320, 1380, 1400, 1440, and 1610 cm^{-1}. These surface formate and carboxylates may be derived from formic acid and the corresponding carboxylic acids during the course of benzene oxidation with ozone, because surface formate was observed when gaseous formic acid was adsorbed on the catalyst in a separate experiment. Thus, benzene is converted to two types of intermediates, weakly bound compounds and strongly bound surface formate and carboxylates on the catalyst in the oxidation reaction. These species needs higher temperatures for the complete decomposition: heating the catalyst from 573 K to 673 K leads to the decomposition of the residual formate and carboxylates with the evolution of large amounts of CO_x. Further heating up to 723 K leads to the complete decomposition of the intermediates on the catalyst surface. The formation ratio of CO to CO_2 decreases with increasing the

heating temperature. This may reflect the different distribution of adsorbed species and/or the oxidation of CO to CO_2 at high temperatures.

MnO_2/Al_2O_3 catalyst used for benzene decomposition can be regenerated by the heat treatment, since time course plots are almost the same for the fresh and used catalysts which had been heated at 723 K in O_2 (Fig. 9). These findings further support that the buildup of the intermediates on the catalyst surface is the dominant cause of severe deactivation.

5. Conclusions

The alumina-supported manganese oxides catalyze the oxidation of benzene to CO_2 and CO by using ozone as the oxidant at room temperature (295 K). Manganese is crucial to obtaining the catalytic activity; however, the rate of benzene oxidation is almost independent of Mn loading level in the range 5–20 wt%. The mole fractions of CO_2 and CO are around 80 and 20%. A strong correlation is observed between the decomposition rate of benzene and that of ozone. A linear relationship is also observed between the amount of CO_x formed and that of ozone decomposed. The catalysts suffer from severe deactivation due to the buildup of these intermediate compounds on the catalyst surface. The poor carbon balance (27–36%) is ascribed to the formation of two types of oxygen-containing intermediates, weakly bound compounds including formic acid, acetic acid, oxalic acid, 2,5-furandione, and phenol and strongly bound species, surface formate and carboxylates. The former compounds are removed by heating the used catalyst in O_2 flow at relatively low temperature (< 573 K). A higher temperature (~ 723 K) is necessary for the complete oxidation of the latter species.

References

[1] P.S. Bailey, Chem. Rev. 58 (1958) 925.
[2] C. Gottschalk, J.A. Libra, A. Saupe, Ozonation of Water and Waste Water, Wiley–VCH, Weinheim, 2000.
[3] R. Atkinson, W.P.L. Carter, Chem. Rev. 84 (1984) 437.
[4] P. Hunter, S.T. Oyama, Control of Volatile Organic Compound Emissions: Conventional and Emerging Technologies, Wiley–Interscience, New York, 2000.
[5] B. Dhandapani, S.T. Oyama, Appl. Catal. B 11 (1997) 129.
[6] S.T. Oyama, Catal. Rev.-Sci. Eng. 42 (2000) 179.
[7] S. Imamura, M. Ikebata, T. Ito, T. Ogita, Ind. Eng. Chem. Res. 30 (1991) 217.
[8] A. Naydenov, R. Stoyanova, D. Mehandjiev, J. Mol. Catal. 98 (1995) 9.
[9] G.J. Hutchings, M.S. Scurrell, J.R. Woodhouse, Appl. Catal. 38 (1988) 157.
[10] K. Hauffe, Y. Ishikawa, Chem. Ing. Techn. 46 (1974) 1053.
[11] D. Andreeva, T. Tabakova, L. Ilieva, A. Naydenov, D. Mehandjiev, M.V. Abrashev, Appl. Catal. A 209 (2001) 291.
[12] A. Naydenov, D. Mehandjiev, Appl. Catal. A 97 (1993) 17.
[13] D. Mehandjiev, K. Cheshkova, A. Naydenov, V. Georgesku, React. Kinet. Catal. Lett. 76 (2002) 287.
[14] D. Mehandjiev, A. Naydenov, G. Ivanov, Appl. Catal. A 206 (2001) 13.
[15] A. Gervasini, G.C. Vezzoli, V. Ragaini, Catal. Today 29 (1996) 449.
[16] M.N. Klimova, B.I. Tarunin, Y.A. Aleksandrov, Kinet. Catal. 26 (1986) 987.
[17] W. Li, S.T. Oyama, Stud. Surf. Sci. Catal. 110 (1997) 873.
[18] A. Gervasini, C.L. Bianchi, V. Ragaini, in: J.N. Armor (Ed.), Environmental Catalysis, in: ACS Symp. Ser., vol. 552, Am. Chem. Society, Washington, DC, 1994, p. 353.
[19] W. Li, G.V. Gibbs, S.T. Oyama, J. Am. Chem. Soc. 120 (1998) 9041.
[20] W. Li, S.T. Oyama, J. Am. Chem. Soc. 120 (1998) 9047.
[21] R. Radhakrishnan, S.T. Oyama, J.G. Chen, K. Asakura, J. Phys. Chem. B 105 (2001) 4245.
[22] R. Radhakrishnan, S.T. Oyama, Y. Ohminami, K. Asakura, J. Phys. Chem. B 105 (2001) 9067.
[23] R. Radhakrishnan, S.T. Oyama, J. Catal. 199 (2001) 282.
[24] R. Radhakrishnan, S.T. Oyama, J. Catal. 204 (2001) 516.
[25] H. Einaga, S. Futamuara, React. Kinet. Catal. Lett. 81 (2004) 121.
[26] F. Kapteijn, A.D. van Langeveld, J.A. Moulijn, A. Andreini, M.A. Vuurman, A.M. Turek, J.-M. Jehng, I.E. Wachs, J. Catal. 150 (1994) 94.
[27] F. Kapteijn, L. Singoredjo, M. van Driel, A. Andreini, J.A. Moulijn, G. Ramis, I.E. Wachs, J. Catal. 150 (1994) 105.
[28] B.R. Strohmeier, D.M. Hercules, J. Phys. Chem. 88 (1984) 4922.
[29] M.A. Baltanas, A.B. Stiles, J.R. Katzer, J. Catal. 88 (1984) 362.
[30] E. Finocchio, G. Busca, Catal. Today 70 (2003) 213.
[31] C. Li, K. Domen, K. Maruya, T. Onishi, J. Catal. 125 (1990) 445.
[32] K. Hirota, K. Fueki, K. Shindo, Y. Nakai, Bull. Chem. Soc. Jpn. 32 (1959) 1261.